THE ePIC EXPERIMENT PHYSICS PROGRAM OVERVIEW*

Mariusz Przybycien

on behalf of the ePIC Collaboration

AGH University of Krakow, al. Mickiewicza 30, 30-059 Kraków, Poland

Received 25 March 2024, accepted 24 June 2024, published online 5 August 2024

The electron–Proton/Ion Collider Experiment (ePIC) Collaboration was formed to design, build, and operate the Electron–Ion Collider (EIC) project detector. Measurements to be performed with ePIC aim to address some of the most profound questions in Quantum Chromodynamics (QCD) related to the emergence of nuclear properties by precisely imaging gluons and quarks inside protons and nuclei. This paper presents an overview of the current configuration of the ePIC detector and its physics program.

DOI:10.5506/APhysPolBSupp.17.5-A29

1. Introduction

On January 9$^{\text{th}}$ 2020, the U.S. Department of Energy announced the selection of Brookhaven National Laboratory (BNL) as the site for the long-planned Electron–Ion Collider (EIC). It is expected that the EIC project will help to find answers to many open questions in QCD [1]: How are the sea quarks and gluons, and their spins, distributed in space and momentum inside the nucleon? How do the nucleon properties, such as mass and spin, emerge from them and their interactions? How do colour-charged quarks and gluons, and colourless jets interact with a nuclear medium? How do the confined hadronic states emerge from these quarks and gluons? How do the quark–gluon interactions create nuclear binding? How does a dense nuclear environment affect the quarks, gluons, their correlations, and their interactions? What happens to the gluon density in nuclei? Does it saturate at high energy, giving rise to a gluonic matter with universal properties in all nuclei, even the proton?

* Presented at the 30$^{\text{th}}$ Cracow Epiphany Conference on *Precision Physics at High Energy Colliders*, Cracow, Poland, 8–12 January, 2024.

To answer those questions, a new machine is needed which will allow for collisions of electrons with protons and light and heavy ions in a broad range of centre-of-mass energies $\sqrt{s} = 20$–140 GeV, providing for high luminosity ($\sim 10^{34}$ cm^{-2}s^{-1}) and allowing for high polarization ($\sim 70\%$) of both the electron and proton (light-ion) beams. The EIC Conceptual Design Report [2] provides a detailed description of the new accelerator.

To perform all considered measurements, a state-of-the-art detector with nearly $4pi$ geometrical coverage, excellent particle identification capabilities, and momentum resolution is needed. In July 2022, the ePIC Collaboration [3] was established to build the EIC project detector.

2. The ePIC detector

The ePIC detector technologies will enable intricate measurements of inclusive and semi-inclusive Deep Inelastic Scattering (DIS), as well as exclusive processes in electron–ion collisions. The ambitious physics goals and the constraints imposed by the challenging collider structure result in the detector design, where several up-to-date and novel detector technologies have been selected. The primary detector needs to cover the range of pseudorapidity $|\eta| < 4$ for the measurement of electrons, photons, hadrons, and jets. It will need to be augmented by auxiliary detectors such as low-Q^2 tagger in the far backward region and proton (Roman pots) and neutron (ZDC) detection in the far forward region. A precise determination of the absolute luminosity with accuracy below 1% will use the bremsstrahlung process [4]. The up-to-date schematic view of the ePIC detector can be found in Ref. [3].

3. Physics program

The physics case for the EIC has been presented in detail in several documents including the EIC White Paper [5] and EIC Yellow Report [1]. The main categories of processes to be studied in the $e + p(A) \rightarrow e + (p, A) + X$ reaction are shown in Fig. 1 and include: inclusive Deep Inelastic Scattering (DIS), semi-inclusive DIS (SIDIS), Deeply Virtual Compton Scattering

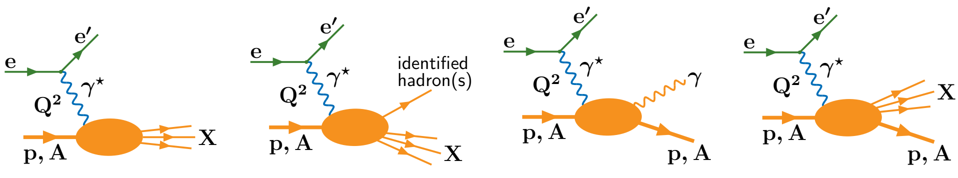

Fig. 1. Main categories of processes to be studied at the EIC, from left: inclusive DIS, semi-inclusive DIS, DVCS, diffractive DIS. For simplicity, only neutral current processes are shown. Usually, $Q^2 \gtrsim 1$ GeV^2 is assumed for DIS. Similar general categories of processes can be considered for photoproduction with $Q^2 \lesssim 1$ GeV^2.

(DVCS), and diffractive-like scattering in which the target proton (or ion) remains intact. Depending on the virtuality of the exchanged photon, the process belongs either to the DIS class (conventionally if $Q^2 \gtrsim 1$ GeV^2) or photoproduction ($Q^2 \lesssim 1$ GeV^2). In addition to the neutral current (NC) diagrams shown in Fig. 1 in which photon (or Z boson) is exchanged, one can also consider charged current (CC) diagrams in which W boson is exchanged and the initial electron converts to the neutrino.

Below we briefly discuss the key measurements to be performed at the EIC, though, the EIC science case is ever-evolving.

3.1. Proton spin

Spin and mass are among the most important quantities that characterize any hadron. The spin of the nucleon can be decomposed to [6, 7]

$$\frac{1}{2} = \frac{1}{2}\int_0^1 \mathrm{d}x\, \Delta\Sigma\left(x, Q^2\right) + \int_0^1 \mathrm{d}x\, \Delta G\left(x, Q^2\right) + \int_0^1 \mathrm{d}x\left(\mathcal{L}_q + \mathcal{L}_g\right), \qquad (1)$$

where $\frac{1}{2}\Delta\Sigma$ (ΔG) are contributions from quark plus anti-quark (gluon) spins, and $\mathcal{L}_q$ ($\mathcal{L}_g$) are contributions from quark (gluon) orbital angular momenta. Presently available results suggest that $\sim 25\%$ of the nucleon spin is carried by the spins of the quarks and anti-quarks, and ΔG is non-zero. However, their values still have very large uncertainties, especially at $x \lesssim 0.01$. Through measurements of polarized DIS, the EIC will provide unprecedented detail of the parton helicity distributions down to $x \sim 10^{-4}$. In Fig. 4 (left), the existing and expected from the EIC measurements of the spin structure function $g_1(x, Q^2)$ are shown. This will not only result in a much better understanding of both $\Delta\Sigma$ and ΔG, but also further constrain the sum $\mathcal{L}_q + \mathcal{L}_g$ in Eq. (1). The expected reduction of statistical uncertainties on the helicity distributions of sea quarks and gluons is shown in Fig. 2. A recent overview of spin physics at the EIC can be found in Ref. [11].

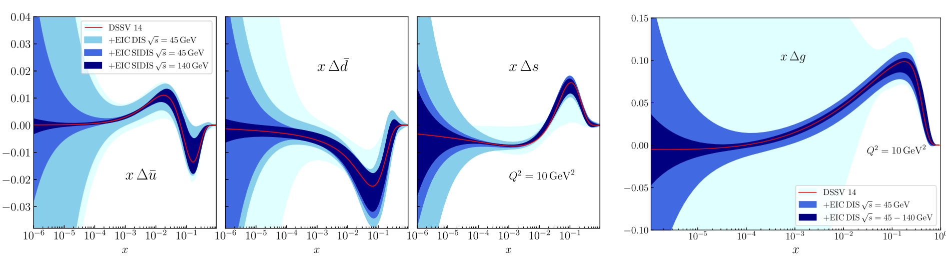

Fig. 2. Expected impact of the EIC SIDIS data on the sea-quark and gluon helicity distributions as functions of x at $Q^2 = 10$ GeV^2. Together with the DSSV14 estimate [9] shown are the uncertainty bands resulting from including the EIC simulated data mentioned in the legend. Plots from Refs. [1, 10].

3.2. Multi-dimensional imaging of nucleons and nuclei

The most general information on the partonic structure of hadrons is contained in the generalized parton distributions (GPDs) and the transverse momentum-dependent parton distributions (TMDs) [12]. These two types of parton distributions provide a complementary 3-dimensional picture of the nucleon, either in a mixed position-momentum representation for the GPDs or in a pure momentum space for the TMDs. They contain also important information on the orbital motion of partons inside the nucleon [13]. While TMDs can be measured in the SIDIS or the Drell–Yan process, GPDs appear in the QCD description of hard exclusive reactions such as DVCS or deeply virtual meson production (DVMP).

Impact parameter distributions (IPDs) can be obtained by taking a Fourier transform of the GPDs in the variable t (at $\xi = 0$) [1]. IPDs represent densities of partons with a given momentum fraction x as a function of the impact parameter, b_{T}. Figure 3 (left) shows the precision that the EIC can provide for imaging of quarks using the Fourier transform of the unpolarized DVCS cross section as a function of t [14].

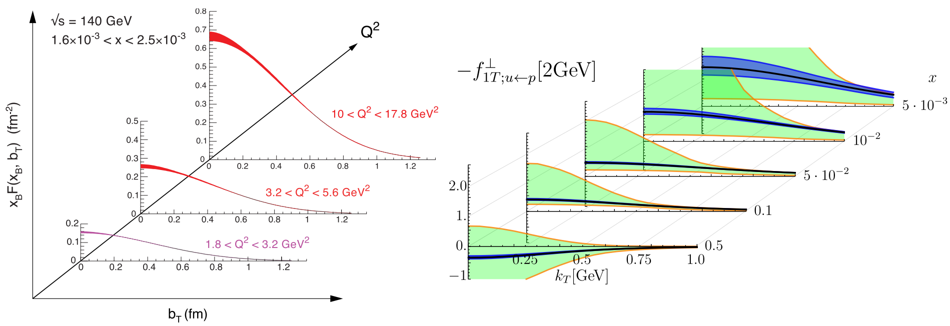

Fig. 3. (Colour on-line) Left: Expected precision of the transverse spatial distribution of partons obtained from the DVCS cross section measured as a function of $|t|$ at the EIC. Shown is the evolution in Q^2 at a fixed x. Taken from Ref. [14]. Right: Expected impact on up quark Sivers distributions as a function of the transverse momentum k_{T} for different values of x, obtained from SIDIS pion and kaon EIC pseudo-data, at the scale of 2 GeV. The green-shaded/light grey areas represent the current uncertainty, while the blue-shaded/dark grey areas are the uncertainties when including the EIC pseudo-data. Taken from [1].

At the EIC, the main access to TMDs comes from SIDIS, where in addition to the standard DIS variables x, Q^2, and y, one also identifies final-state hadrons with fractional energy z and transverse momentum P_{T} relative to the direction of the virtual photon. As shown in Fig. 3 (right), the uncertainty bands can be reduced by more than an order of magnitude, for all flavours [1]. Measuring the P_{T} dependence of the cross section for a given (x, z, Q) bin allows for the determination of the k_{T} shape of the Sivers function, which is currently hardly constrained at all by experimental data.

3.3. Study of the nucleus and gluon saturation

The EIC will be the world's first dedicated electron–nucleus collider and it will address a broad program of fundamental physics with light and heavy nuclei. For a quantitative estimate of the kinematical range accessible in electron–ion collisions, a collection of simulated $e+\mathrm{Au}$ DIS reduced cross sections at three different $\sqrt{s}$ is shown if Fig. 4 (right). The projected uncertainties include those implemented in the EPPS16 model [15]. For comparison, the current world data on DIS off heavy ions are also shown.

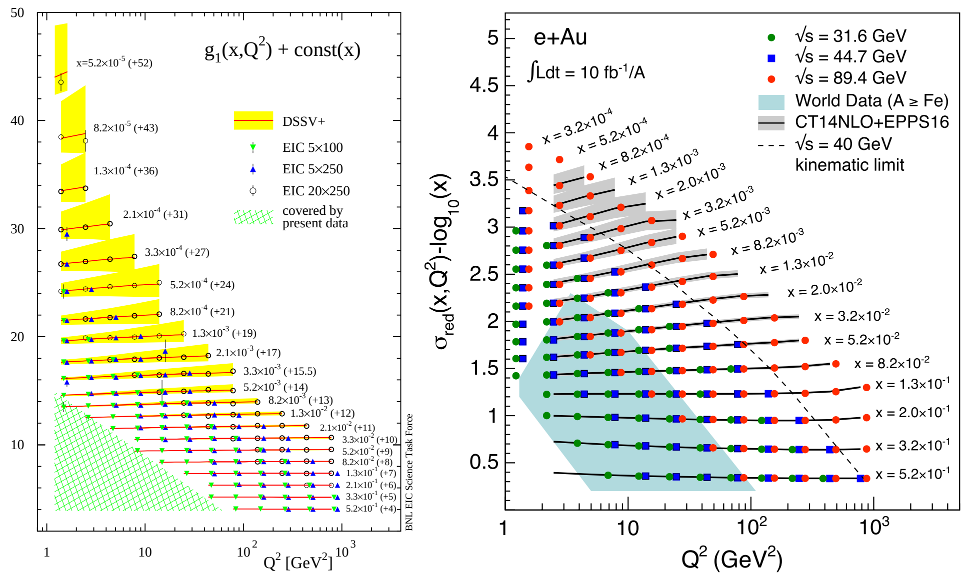

Fig. 4. Left: Projected EIC pseudo-data for the spin structure function of the proton $g_1(x, Q^2)$ for three different combinations of electron and proton energies. Taken from [8]. Right: Reduced cross sections plotted as a function of Q^2 and x for inclusive EIC pseudo-data from $e+\mathrm{Au}$ collisions at several centre-of-mass energies and the EPPS16 model [15]. Taken from [14].

Due to the rapid rise with the energy of the gluon density in hadrons, gluons play a key role in our understanding of DIS and hadronic collisions at high energies. DIS experiments on heavy nuclei at high energies are ideally suited for the study of non-linear gluon dynamics. The projectile interacts coherently with a large number of stacked nucleons. This probes very strong colour fields at high energy, which is expected to lead to gluon saturation, described by an effective theory known as the Colour Glass Condensate (CGC) [16].

Thanks to $e + A$ collisions with large nuclei, the EIC will reach the saturation regime faster than with ep collisions at similar $\sqrt{s}$. As shown in Fig. 5 (left), the saturation scale Q_s is expected to scale with the ion-mass number A as $Q_\mathrm{s}^2 \sim A^{1/3}x^{-\lambda}$. The EIC will investigate the onset of saturation, explore its properties and reveal its dynamical behaviour.

To directly probe the Weizsäcker–Williams (WW) gluon distribution and gluon saturation effects at low x, one can measure the azimuthal angle difference, $\Delta\phi$, between two back-to-back charged hadrons (or jets)

$$C(\Delta\phi) = \frac{\mathrm{d}\sigma(\gamma^\star + A \to h_1 + h_2 + X)}{\mathrm{d}z_1\,\mathrm{d}z_2\,\mathrm{d}\Delta\phi} \Big/ \frac{\mathrm{d}\sigma(\gamma^\star + A \to h_1 + X)}{\mathrm{d}z_1\,\mathrm{d}\Delta\phi}\,. \tag{2}$$

These correlations are sensitive to the transverse momentum dependence of the gluon distribution. Due to saturation, the WW gluon TMD can provide additional transverse momentum broadening to the back-to-back correlation causing the disappearance of the away-side peak when saturation is overwhelming. In Fig. 5 (right), the ratios of the correlation functions in e + Au over those in ep are shown for three energies. The suppression increases with energy. The precise measurement of dihadron correlations will allow us not only to determine whether the saturation regime has been reached but also to study the non-linear evolution of spatial multi-gluon correlations.

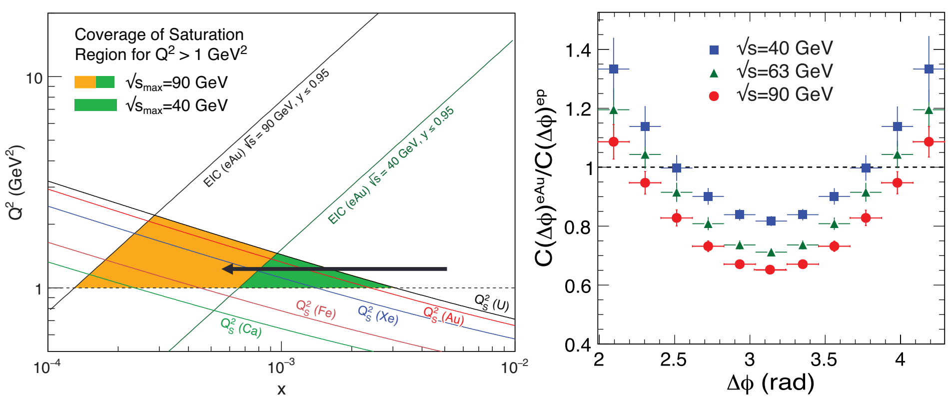

Fig. 5. Left: The kinematic reach in x and Q^2 of the EIC for different electron beam energies, given by the regions to the right of the diagonal black lines, compared with predictions of the saturation scale, Q_s^2, for different heavy-ion species. Right: The ratio of the dihadron correlation functions in e+Au and ep for three centre-of-mass energies. Taken from [14].

The *ep* DIS experiments provided detailed information on the proton structure allowing extraction of very accurate parton distribution functions (PDFs) inside the proton. It is expected that the structure of nucleons inside nuclei is modified. These nuclear PDFs (nPDFs) will be measured in $e + A$ DIS experiments at the EIC in a broad kinematical range and with much better precision than currently available. It will be possible to obtain a direct constraint of the gluon density by measuring heavy flavour pairs which at LO are produced through the photon–gluon fusion process.

3.4. Diffraction at the EIC

Diffractive interactions result when the electron probe in DIS interacts with a proton or nucleus by exchanging several partons with zero net colour, referred to as Pomeron. At the EIC energy regime, diffractive processes are expected to share a large ($> 30\%$) fraction of the total cross section and nuclear diffractive structure functions will be a sensitive saturation measurement [17]. Diffractive processes are most sensitive to the underlying gluon distribution and give access to the spatial distribution of gluons in nuclei. The reason for this sensitivity is that the diffractive structure functions depend, in a wide kinematic range, quadratically on the gluon momentum distribution and not linearly as in DIS. Diffractive events are characterized by a rapidity gap, *i.e.* an angular region in the direction of the scattered proton or nucleus without particle flow. Detecting events with rapidity gaps requires a largely hermetic detector.

The production of vector mesons (VM) in diffractive processes, $e + A \to e + A + V$, where $V = J/\Psi, \phi, \rho$ is a unique process, for it allows the measurement of the momentum transfer, t, at the hadronic vertex where four momentum of the outgoing nuclei cannot be measured [1, 18]. Since only one new final-state particle is produced, the process is experimentally clean and can be unambiguously identified by the presence of a rapidity gap. The study of various VM in the final state allows for a systematic exploration of the saturation regime. The J/Ψ is the vector meson least sensitive to saturation effects due to the small size of its wave function. Larger mesons such as ϕ or ρ are considerably more sensitive to saturation effects.

Figure 6 shows the differential cross section as a function of t for J/Ψ and ϕ mesons production. The coherent distribution depends on the shape of the source while the incoherent distribution provides valuable information on the fluctuations of the source [19]. As the J/Ψ is smaller than the ϕ, one sees little difference between the saturation and no-saturation scenarios for exclusive J/Ψ production but a pronounced effect for the ϕ. The coherent distributions can be used to obtain information about the gluon distribution in impact parameter space $F(b)$ through a two-dimensional Fourier transform:

$$F(b) = \int_0^\infty \frac{\mathrm{d}q\, q}{2\pi} J_0(qb) \sqrt{\frac{\mathrm{d}\sigma_{\mathrm{coherent}}}{\mathrm{d}t}} \,. \tag{3}$$

The EIC will be able to obtain the nuclear spatial gluon distribution from the measured coherent t spectrum from exclusive J/Ψ and ϕ production in $e + A$ collisions, in a model-independent way.

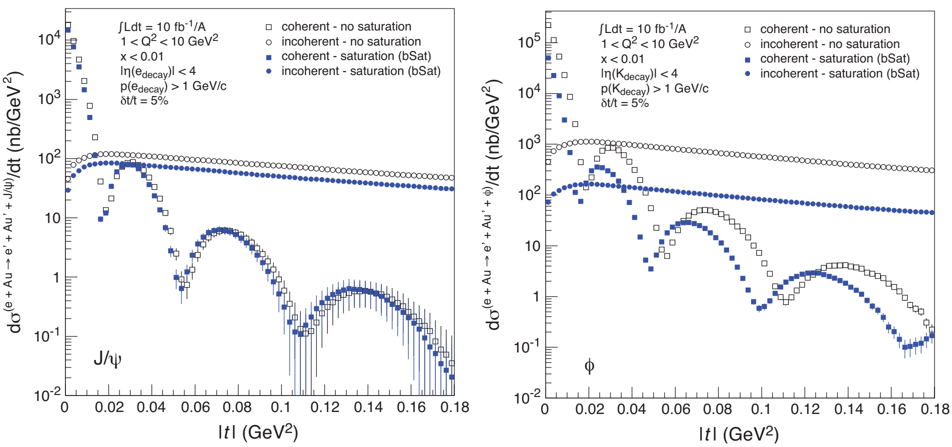

Fig. 6. Differential cross sections for the exclusive production of J/Ψ (left) and ϕ (right) mesons production in coherent and incoherent events in diffractive $e + \mathrm{Au}$ collisions. Predictions from saturation and non-saturation models are also shown. Taken from [5].

4. Summary and the future perspective

The EIC will be the world's first electron–nucleus and polarized electron–polarized proton (light ion) collider. The lepton–proton/ion scattering provides information on nucleon structure complementary to hadron–hadron collisions. The upcoming EIC will significantly deepen our knowledge of several aspects of the nucleon structure by allowing for performing new measurements in a broad range of x and Q^2 and significantly reduce uncertainties in the existing measurements. The EIC scientific case is still evolving and new ideas have been proposed, see *e.g.* [20–22].

The ongoing studies related to the ePIC detector are expected to be finalized with a TDR at the beginning of 2025. Work on constructing the new accelerator and detector will begin in 2026, after the experiments at RHIC finish data-taking in late 2025. The first data from the ePIC experiment are expected in 2032.

It is worth mentioning that studies of a polarized Electron-ion collider in China (EicC) are also ongoing [23]. It is expected that EicC will be complementary to the EIC-US and operate at lower centre-of-mass energies.

REFERENCES

[1] R. Abdul Khalek *et al.*, *Nucl. Phys. A* **1026**, 122447 (2022), arXiv:2103.05419 [physics.ins-det].

[2] J. Adam *et al.*, EIC CDR.

[3] ePIC webpage https://wiki.bnl.gov/EPIC/index.php?title=Main_Page

[4] K. Piotrzkowski, *J. Instrum.* **16**, P09023 (2021), arXiv:2106.08993 [physics.acc-ph].

[5] A. Accardi *et al.*, *Eur. Phys. J. A* **52**, 268 (2016), arXiv:1212.1701 [nucl-ex].

[6] R.L. Jaffe, A. Manohar, *Nucl. Phys. B* **337**, 509 (1990).

[7] X. Ji, F. Yuan, Y. Zhao, *Nat. Rev. Phys.* **3**, 27 (2021), arXiv:2009.01291 [hep-ph].

[8] E.C. Aschenauer *et al.*, *Phys. Rev. D* **86**, 054020 (2012), arXiv:1206.6014 [hep-ph].

[9] D. de Florian, R. Sassot, M. Stratmann, W. Vogelsang, *Phys. Rev. Lett.* **113**, 012001 (2014), arXiv:1404.4293 [hep-ph].

[10] I. Borsa *et al.*, *Phys. Rev. D* **102**, 094018 (2020), arXiv:2007.08300 [hep-ph].

[11] M. Zurek, *Acta Phys. Pol. B Proc. Suppl.* **16**, 7-A3 (2023).

[12] M. Diehl, *Eur. Phys. J. A* **52**, 149 (2016), arXiv:1512.01328 [hep-ph].

[13] M. Burkardt, *Few Body Syst.* **58**, 137 (2017).

[14] E.C. Aschenauer *et al.*, *Rep. Prog. Phys.* **82**, 024301 (2019), arXiv:1708.01527 [nucl-ex].

[15] K.J. Eskola, P. Paakkinen, H. Paukkunen, C.A. Salgado, *Eur. Phys. J. C* **77**, 163 (2017), arXiv:1612.05741 [hep-ph].

[16] F. Gelis, E. Iancu, J. Jalilian-Marian, R. Venugopalan, *Annu. Rev. Nucl. Part. Sci.* **60**, 463 (2010), arXiv:1002.0333 [hep-ph].

[17] M.S. Kugeratski, V.P. Goncalves, F.S. Navarra, *Eur. Phys. J. C* **46**, 413 (2006), arXiv:hep-ph/0511224.

[18] M. Lomnitz, S. Klein, *Phys. Rev. C* **97**, 015203 (2019), arXiv:1803.06420 [nucl-ex].

[19] H. Kowalski, T. Lappi, C. Marquet, R. Venugopalan, *Phys. Rev. C* **78**, 045201 (2008), arXiv:0805.4071 [hep-ph].

[20] R. Abdul Khalek *et al.*, arXiv:2203.13199 [hep-ph].

[21] B.S. Page, X. Chu, E.C. Aschenauer, *Phys. Rev. D* **101**, 072003 (2020), arXiv:1911.00657 [hep-ph].

[22] J.J. Chwastowski, K. Piotrzkowski, M. Przybycien, *Eur. Phys. J. C* **82**, 846 (2022), arXiv:arXiv:2206.02466/hep-ph.

[23] D.P. Anderle *et al.*, *Front. Phys.* **16**, 64701 (2021), arXiv:2102.09222 [nucl-ex].